Journal of Environment & Biotechnology Research
VINANIE PUBLISHERS
www.vinanie.com/jebr

Artificial neural network approach for modelling of methyl violet 2B dye adsorption using pomelo skin

Muhammad Khairud Dahri, Muhammad Raziq Rahimi Kooh,* Linda Biaw Leng Lim

Chemical Sciences, Faculty of Science, Universiti Brunei Darussalam, Jalan Tungku Link, Gadong, Negara Brunei Darussalam

ORIGINAL RESEARCH ARTICLE

ABSTRACT

This study investigates pomelo peel (PP) as a low-cost adsorbent for removal of methyl violet 2B (MV) by batch adsorption study. The adsorbent was characterised using Fourier-transform infrared spectroscopy. The experiments included the effects of pH, ionic strength, temperature, initial dye concentration and contact time. Modelling of the adsorption process with a three-layer artificial neural network were in good agreement with the experimental data with high correlation coefficient (R=0.9978) and low error (root mean square error =0.01) for 3 neurons in the hidden layer. The data on the investigation of ionic strength (62% dye removal at 0.8 mol/L KNO_3) showed that hydrophobic-hydrophobic interaction may be the dominant force of attraction between the adsorbent and adsorbate, as the electrostatic interaction was suppressed at high salt concentration. The pseudo second model best described the adsorption kinetics as the adsorption followed a second order rate law with respect to availability of adsorption sites. The Weber-Morris intraparticle diffusion model indicated that the rate-limiting step was not intraparticle diffusion. Thermodynamics study revealed that PP-MV adsorption system was spontaneous and exothermic in nature. Lastly, the Langmuir model best represented the adsorption process and predicted a superior qmax value of 1.2 mmol/g (468.3 mg/g).

KEYWORDS

Adsorption; Artificial neural network; Methyl violet 2B; Pomelo peel; Water remediation

1. INTRODUCTION

The past decades have seen a growing need of the world for restoring and protecting the environment from pollutants that can affect soil, air and water. Man-made pollutants are direct and/or indirect cause of wastes from industries that demanded 'zero discharge' policy (Wang et al., 2010). As such, various treatments were engineered based on the basic principles of chemistry, biology, microbiology, mathematics and physics of the wastes i.e. adsorption (Kooh et al., 2016c), phytoremediation (Lim et al., 2016), precipitation (Kooh et al., 2017b), ozonation (Langlais et al., 1991), photocatalytic (Chong et al., 2010) and electrochemical (Peralta-Hernández et al., 2006), where their advantages and disadvantages have been widely covered in literature (Vijayaraghavan, 2016; Kooh et al., 2016e; Crini, 2006). Many methods may be effective, however some of the downside may include high cost of treatment, production of sludge or production of toxic intermediate compounds (Crini, 2006). Thus, finding alternative methods that are cheaper, safer and environmental friendly is always encouraged.

Adsorption is a surface phenomenon which involves the adhesion of ions, molecules or atoms onto a solid surface and can be classified as a physisorption (van der Waals forces) or chemisorption (covalent bonding) process. Using this simple concept, activated charcoal is commonly used to adsorb pollutants (Bansal and Goyal, 2005) and in recent decades, various materials such as hen feathers, kaolinite and montmorillonite have been studied for their potentials

Corresponding author: **M.R.R. Kooh**
Tel: +673 8658876
Fax: +673 2461502
E. mail: chernyuan@hotmail.com

Received: 10-04-2017
Revised: 30-05-2017
Accepted: 05-06-2017
Available online: 01-07-2017

as adsorbents (Demirbas, 2008; Bhattacharyya and Gupta, 2008). Some of the advantages of using adsorption method are that it is cheap, simple, has no side product formation and the used adsorbents can be easily collected and reused (Kooh et al., 2016g). Adsorption can also be easily scaled up and adopted by industry to treat their wastewater.

Pomelo (*Citrus maxima*), also known as shaddock, is a natural citrus fruit that is native to Southeast Asia with an appearance similar to a large grapefruit. The fruit has pale green to yellow coloured peel when ripe with thick rind pith and has white edible flesh. The fruit's peel can be candied and made into marmalade. However due to its large production, large amount of the peel (around 270 to 500 tonnes) is being discarded as waste annually (Liang et al., 2012). Considering its abundance, pomelo peel is an attractive material to be used as a low cost adsorbent. Moreover, it has porous and spongy structure (Liang et al., 2012) which can be advantageous in the adsorption process. Its potential as an adsorbent can be seen in various studies (Tasaso, 2014; Luo et al., 2010; Saikaew et al., 2009; Argun et al., 2014; Foo and Hameed, 2011; Hameed et al., 2008; Dahri et al., 2017b).

In this study, pomelo peel (PP) is utilised as an adsorbent to remove toxic methyl violet 2B (MV) dye from aqueous solution. The effects of contact time, pH, ionic strength, temperature and various dye concentrations were investigated. The experimental data were fitted into various models in order to further understand the adsorption of MV onto PP. A mathematical model, artificial neural network (ANN), was also applied to predict adsorption behaviour based on the experimental data.

ANN is a form of machine learning algorithm inspired from the function of a biological neuron. It is also one of the best strategies used in the modelling of environmental and pollution research due to its robustness and capability to deal with noisy data, yet able to predict data with reasonable accuracy. In general, ANN works by feeding the model with experimental data as inputs, where the algorithm processed the data by assigning weights to the collection of inputs and threshold of the results. Once the model is trained, it can predict the outcome. ANN have been used in the modelling of phytoextraction of malachite green using live *Azolla pinnata* with correlation coefficient of 0.867 (Kooh et al., 2016f), and adsorption of methyl violet 2b using soya bean waste which reported correlation coefficient of 0.995, where high correlation coefficient indicates good predictive performance (Kooh et al., 2016d).

2. MATERIALS AND METHODS

2.1. Chemical and instrumentation

Methyl violet 2B ($C_{24}H_{28}N_3Cl$; Mr: 393.95 g/mol) and potassium nitrate were purchased from Sigma-Aldrich. The solution pH was adjusted using NaOH (Univar) and HNO_3 (AnalaR). Fourier Transform Infrared spectroscopy (FTIR) analysis using Shimadzu IR Prestige-21 spectrophotometer was done using pellet method made from spectroscopy grade KBr (Sigma-Aldrich). Panasonic MX-J210GN blender was used to blend the sample and a Gallenkamp Hotbox oven was used for drying purposes. Solution mixtures were agitated using Stuart orbital shakers and Orion 2 Star pH Benchtop digital pH meter (Thermo Scientific) was used to measure the solution pH. A single beam UV-vis Jenway 6320D (UV-vis) spectrophotometer was used for analysis of MV at wavelength 584 nm.

2.2. Preparation of sample and working solutions

Pomelo peel (PP) was separated from the fruit's flesh and was dried in an oven at 70 °C until a constant mass was obtained. The dried PP was then blended into powder and sieved in order to obtained particle size of 355 – 850 μm. The sample was stored in an airtight plastic bag.

Stock solution of MV was prepared by dissolving an appropriate amount of MV powder in a known volume of distilled water. All lower dye concentrations were obtained by serial dilution of the stock solution of MV. The stock solution of KNO3 was prepared and diluted to lower concentrations using the same method.

2.3. Experimental procedure

The general procedure for the adsorption study was done by mixing PP (0.04 g) with a known concentration of MV (20.0 mL) and the mixture was agitated at 250 rpm for 2 h. The filtrate was collected and the dye content was measured using UV-vis. The parameters included in this study were the effects of contact time (time interval from 5 – 240 min), pH (3, 4, 6, 8 and 10), ionic strength (0, 0.01, 0.10, 0.20, 0.40, 0.60 and 0.80 mol/L KNO_3), temperature (25, 40, 50, 60 and 70 °C) and initial dye concentration (10, 20, 40, 60, 80, 100, 200, 300, 400, 500, 600, 800 and 1000 mg/L). All experiments were done in duplicate.

The amount of dye adsorbed per gram of PP, q_e (mmol/g) and percentage removal (%) were calculated using equation 1 and equation 2, respectively.

$$q_e = \frac{(C_i - C_e)V}{mM_r} \quad (1)$$

$$\text{Percentage removal} = \frac{(C_i - C_e)\times 100\,\%}{C_i} \quad (2)$$

where C_i is the initial dye concentration (mg/L), C_e is the equilibrium dye concentration (mg/L), V is the volume of dye solution used (L), M_r is the molecular mass of MV (g/mol) and m is the mass of PP used (g).

2.4. Kinetics models

The experimental data on contact time was fitted into the Lagergren first order (Lagergren, 1898), pseudo second order (Ho and McKay, 1998) and Weber Morris intra-particle diffusion (Weber and Morris, 1963) models as shown below:

Lagergren first order:

$$\log (q_{e,cal} - q_t) = \log q_{e,cal} - \frac{t}{2.303} k_1 \quad (3)$$

Pseudo second order:

$$\frac{t}{q_t} = \frac{1}{q_{e,cal}{}^2 k_2} + \frac{t}{q_{e,cal}} \quad (4)$$

Weber Morris intra-particle diffusion:

$$q_t = k_3\, t^{1/2} + C \quad (5)$$

where t is the agitation time (min), q_t is the adsorbate adsorbed per gram of PP (mmol/g) at time t, k_1 is the Lagergren first order rate constant (min^{-1}), k_2 is pseudo second order rate constant (g/mmol min), k_3 is the intraparticle diffusion rate constant (mmol/g $min^{1/2}$) and C is the slope that represents the thickness of the boundary layer.

2.5. Isotherm models

Similarly, the experimental data on the effect of dye concentration was fitted into the Langmuir (Langmuir, 1918), Freundlich (Freundlich, 1906) and Sips (Sips, 1948) isotherm models as shown below:

Langmuir:

$$\frac{C_e}{q_e} = \frac{1}{b\, q_{max}} + \frac{C_e}{q_{max}} \quad (6)$$

Freundlich:

$$lnq_e = \frac{1}{n_F} lnC_e + lnK_F \quad (7)$$

Sips:

$$\ln\left(\frac{q_e}{q_{max} - q_e}\right) = \frac{1}{K_{LF}} lnC_e + lnK_s \quad (8)$$

where q_{max} (mmol/g) is the maximum adsorption capacity, b (L/mmol) is the Langmuir constant, K_F (mmol/g) is the adsorption capacity, n_F value (between 1 and 10) indicates favourability of the adsorption process, K_S (L/g) is the Sips constant and K_{LF} is the exponent.The separation factor (R_L) is a dimensionless constant that uses the Langmuir model's constant to gauge the favourability of the adsorption process. It is given by the following equation:

$$R_L = \frac{1}{(1 + bC_o)} \quad (9)$$

where C_o (mg/L) is the highest initial dye concentration. The adsorption process is either unfavourable ($R_L > 1$), linear ($R_L = 1$), favourable ($0 < R_L < 1$), or irreversible ($R_L = 0$).

2.6. Statistical analysis

Correlation coefficient of determination (R^2) value and error analyses such as the sum of absolute error (EABS) and the chi-square test (χ^2) (Foo and Hameed, 2010) were used to evaluate the similarity of the calculated values with that of the experimental data.

$$\text{EABS} = \sum |q_i - Q_i| \quad (10)$$

$$\chi^2 = \sum_{i=1}^{j} \frac{(Q_i - q_i)^2}{q_i} \quad (11)$$

where Q_i is the experimental value while q_i is the calculated value and j is the number of observations in the experiment. The smaller the EABS and χ^2 values, the better the correlation between the calculated values from various models with the experimental data.

2.7. Artificial neural network

The artificial neural network modelling for the

adsorption of MV using PP was carried out using data mining software, Weka version 3.6 (Hall et al., 2009), following the procedures of our previous study (Kooh et al., 2016d) using the classifier "multilayer perceptron". A three-layer model was built consisting of the input layer, hidden layer and output layer. The input layer consists of four neurons (pH, initial adsorbate concentration, temperature and contact time), while the output layer consists of only one neuron (adsorption capacity). In this study, a total of 78 data was used for training the ANN model. All the data was normalised to value of 0 to 1, using equation 12.

$$X_N = \frac{(X_i - X_{min})}{(X_{max} - X_{min})} \quad (12)$$

where X_i is the value of a specific neuron obtained experimentally, XN is the value after been normalised, and Xmax and Xmin are the maximum and minimum value of the experimental data, respectively. The obtained predicted ANN output was then converted back to their original scale.

The number of neurons in the hidden layer needs to be optimised, which was achieved by running a 10-fold "cross-validation", where the input data was randomly divided into training set (90%) and test and validation set (10%) and the process was repeated for 10 times, with each time a different segment was tested. The optimised number of neurons in hidden layer was chosen based on the correlation coefficient (R) and root square mean error (RMSE), generated by the Weka software.The closer the value of R to 1.0 indicated the closer the experimental data to the ANN predicted data, while the lower the value of RMSE indicates lower variation.

3. RESULTS AND DISCUSSION

3.1 Characterisations of the adsorbent

The functional groups present on surface of the PP before and after MV adsorption were analysed using FTIR and shown in Figure 1. For the untreated PP, the band present at 3345 cm^{-1} represents the hydroxyl (-OH) and/or amino (-NH) groups while methyl (CH) group is represented at 2928 cm^{-1}. At 1743 cm^{-1}, carbonyl (C=O) group is clearly seen along with NH bending at 1629 cm^{-1}. After MV adsorption, the adsorbent showed shifts of bands to 3366, 2926, 1726 and 1647 cm^{-1} suggesting the involvement of these functional groups in the adsorption of MV onto the PP's surface. Additionally, three new peaks were observed in the spectrum of MV treated PP: 1514 cm^{-1} ($-COO^-$ anti-symmetric stretching), 1369 cm^{-1} ($-COO^-$ symmetric stretching) and 1157 cm^{-1} (C-N stretching). These peaks were similarly found in our previous study on the adsorption of MV onto soyabean waste (Kooh et al., 2016d).

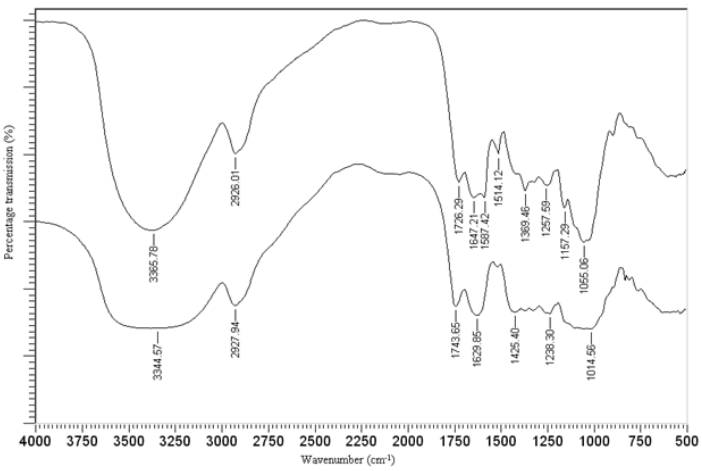

Figure 1. The FTIR spectra of MV treated PP (top) and untreated PP (bottom).

3.2 Artificial neural network (ANN)

The framework of the three-layer ANN model used for modelling the adsorption of MV using PP is represented in Figure 2A. The best performing ANN model is determined by the number of neurons in the hidden layer which resulted in the higher R and the lowest RMSE. As seen in Figure 2B, when no hidden layer is involved the R value is lower, while the RMSE is higher. However, the inclusion of a neuron in the hidden layer resulted in tremendous improvement of both the R and RMSE values. The optimised ANN model is obtained with 3 neurons in hidden layer which has the highest R and lowest RMSE. The variation between the experimental data and the ANN predicted data can be observed in Figure 2C. The overall performance of the ANN model is in good agreement. The comparison of the experimental data and ANN data will be discussed in individual sections.

3.3 Effects of pH and ionic strength

One of the most important parameters in adsorption study is pH as real wastewaters usually have varying pH values. Therefore, it is imperative to investigate how the pH will affect the adsorption process as it can affect the ionisation of functional groups on both the adsorbate and adsorbent (Hanafiah et al., 2012). The

point of zero charge (pH_{pzc}) of PP was found to be at pH 3.53 (Dahri et al., 2017b). Thus, above this value, the surface of PP would be predominately negative in charge due to the deprotonation of functional groups such as carboxyl and hydroxyl groups. Whereas, if the pH falls below the pH_{pzc} value, the surface would be predominately positive in charge due to the protonation of the functional groups such as amino group. If pH is the same as pH_{pzc}, the net charge of the PP is zero.

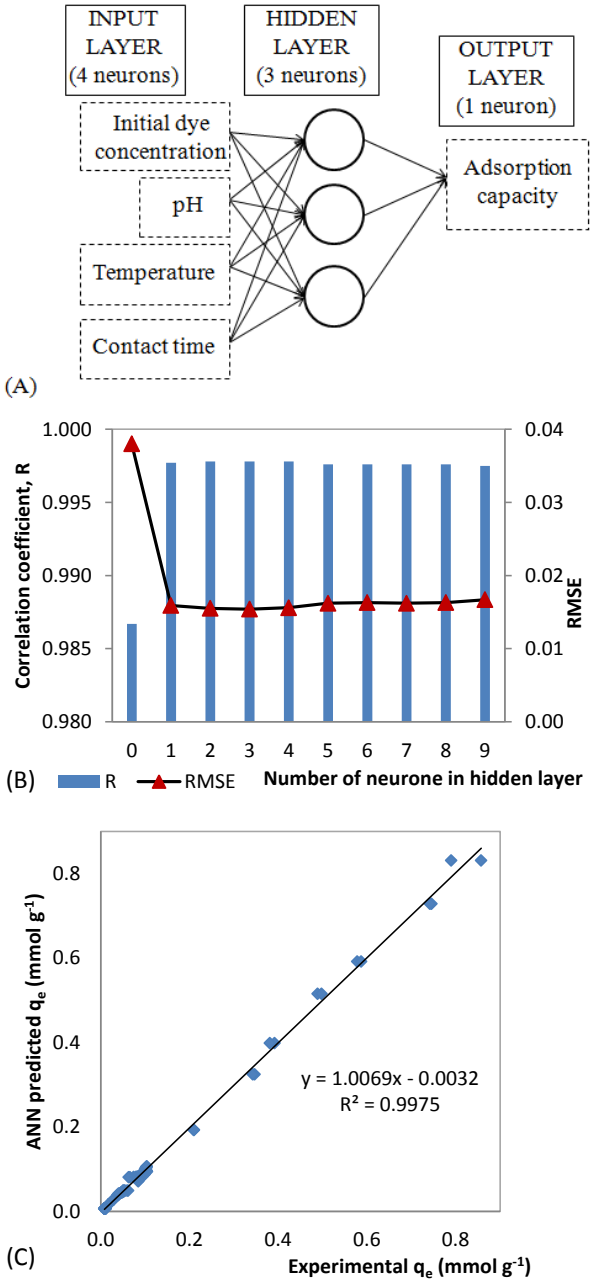

Figure 2. (A) The structure of the ANN model used in this study, graphs showing (B) performance of the ANN models at different number of neurons in the hidden layer, and (C) the closeness between the ANN-predicted data and the experimental data.

From Figure 3A, it can be observed that pH range from 3 to 6 resulted in dye removal at approximately 0.01 mmol/g, whereas at pH 8 a decrease in dye removal was observed. This is in good agreement with the concept of point of zero charge, as aqueous pH above 3.0 resulted in predominantly negatively charged surface which attracts the cationic MV dye by electrostatic interactions. The decrease in dye adsorption at pH 8 or higher is most likely an error due to alkaline fading of the dye resulted in decrease of dye intensity (Samiey and Toosi, 2010; Kooh et al., 2015) which was also observed in other basic dyes such as malachite green (Dahri et al., 2014). The ANN model slightly underestimated the level of MV dye adsorption using PP due to the effect of pH, however it successfully predicted the overall pattern.

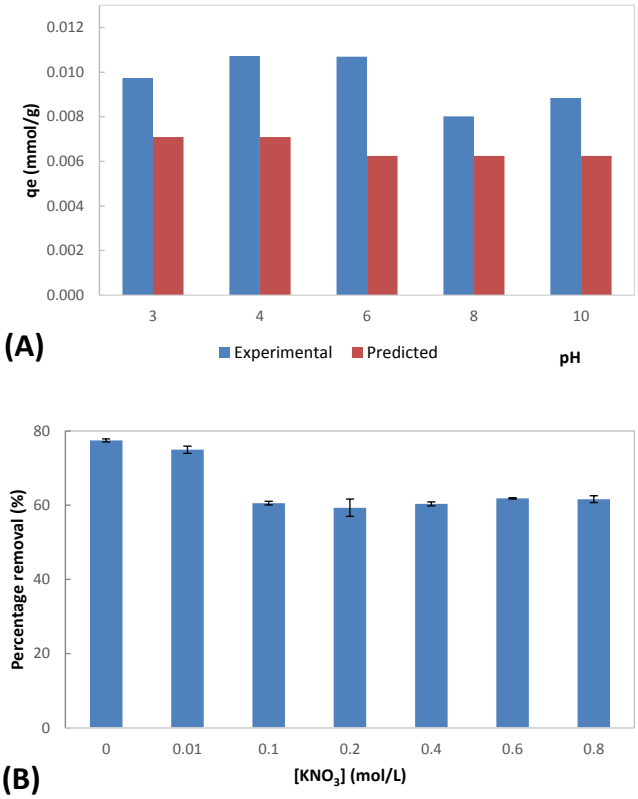

Figure 3. The effect of the (A) pH and (B) KNO_3 concentration for the removal of MV using PP.

The effect of ionic strength on the adsorption of MV using PP is as shown in Figure 3B. Low concentration of KNO_3 (0.01 mol/L) resulted in 75% dye removal which was slightly lower when compared to dye adsorption without KNO_3 (77%). As the KNO_3 concentration increased, the dye removal further decreased, where at 0.8 mol/L KNO_3, the dye removal was at 62%. This behaviour is also observed in removal of other basic dyes such as malachite green and

rhodamine B (Kooh et al., 2016g; Kooh et al., 2016e) and is due to the competition of the salt (K^+) with the cationic MV molecules for the adsorption sites, thereby suppressing the electrostatic interaction (Hu et al., 2013). Despite the suppression of electrostatic interaction, 62% dye removal at 0.8 mol/L KNO_3 also signifies that the adsorbate-adsorbent interaction may occur predominantly by hydrophobic-hydrophobic interaction which is the attraction between the non-polar groups of the adsorbate with the non-polar functional groups on the adsorbent's surface (Hu et al., 2013). ANN was not included for the effect of pH as majority of the batch adsorption experiment did not involve addition of KNO_3.

3.4 Effect of contact time and kinetics study

Investigation of the adsorption's contact time is important as it shows the length of time required for the adsorption process to reach equilibrium. This information is particularly useful when scaling up for treatment of industrial wastewater which is usually in huge volume, and any extra time spend after adsorption reaches equilibrium is not only a waste of time but incur higher cost. As shown in Figure 4A, the dye uptake for the first 30 min was rapid i.e. 0.06 mmol/g (5 min) to 0.09 mmol/g (30 min) and reached equilibrium from 60 min onwards. The rapid uptake is due to the availability of PP's active sites for the dye to interact with, which then slowed down as the sites became saturated with the dye. For the rest of the experiments in this study, contact time of 2 h was used in order to ensure complete equilibrium is attained. As seen in Figure 4A, the ANN model only predicted well for the effect of contact time at time duration beyond 120 min. This is probably due to small amount of data available at shorter shaking time.

Kinetics study is useful as it can give insight on the rate of the adsorption process and the factors affecting the reaction rate (Renault et al., 2008). As such, two kinetics models namely the Lagergren first order and pseudo second order were used for this purpose. These two models were compared with each other in order to determine the best model to describe the adsorption process (Figures 4B&C). Comparing the R^2 and q_e values (Table 1), it can be said that the pseudo second order has better correlation with the experimental data where its R^2 value is higher (1.000), and the calculated q_e ($q_{e,cal}$) (0.104 mmol/g) is in close agreement with the experimental q_e ($q_{e,expt}$) (0.103 mmol/g) compared to the Lagergren first order model. The Lagergren first order model, in many cases, is only applicable to a certain range of time of the adsorption process and is therefore not useful to describe the whole time range (Taty-Costodes et al., 2003). Thus, the model gave lower R^2 values and its $q_{e,cal}$ greatly deviated from the $q_{e,expt}$ value. The pseudo second order model suggests that the adsorption process is dependent on the amount of adsorbate and the availability of the adsorbent's active sites (Fernandes et al., 2007).

Unlike the two previous models, the Weber-Morris intraparticle diffusion model can be used to give insight on the adsorption's diffusion mechanism. When the Weber-Morris plot is linear and passes through the origin, then the intraparticle diffusion is considered as the rate limiting step. In other cases, multi-linear plots can also be obtained as seen in Figure 4D where each linear line represents different stages of the adsorption process. Usually, three stages can be seen in the multi linear plot: 1) fast external diffusion which occurs at the beginning of the process and completed within 5 min and therefore usually absent from intraparticle diffusion plot due to its rapid process; 2) the intraparticle diffusion which is represented by the first linear region (Figure 4D), and 3) the slow equilibrium stage which represented as a plateau (Özacar and Şengil, 2004). From Table 1, the value of C which represents the y-intercept is not zero and therefore, it can be said that intraparticle diffusion is not the rate limiting step in the adsorption of MV onto PP.

Table 1. The kinetics parameters for the adsorption of 100 mg/L MV onto PP

Lagergren first order		**Pseudo second order**		**Weber-Morris Intraparticle diffusion**	
$q_{e,\,expt}$ (mmol/g)	0.103	$q_{e,\,expt}$ (mmol/g)	0.103	k_3(mmol/g $min^{1/2}$)	0.008
$q_{e,\,cal}$ (mmol/g)	0.023	$q_{e,\,cal}$ (mmol/g)	0.104	C	0.047
k_1(1/min)	0.014	k_2(g /mmol min)	2.323		
R^2	0.864	R^2	1.000		

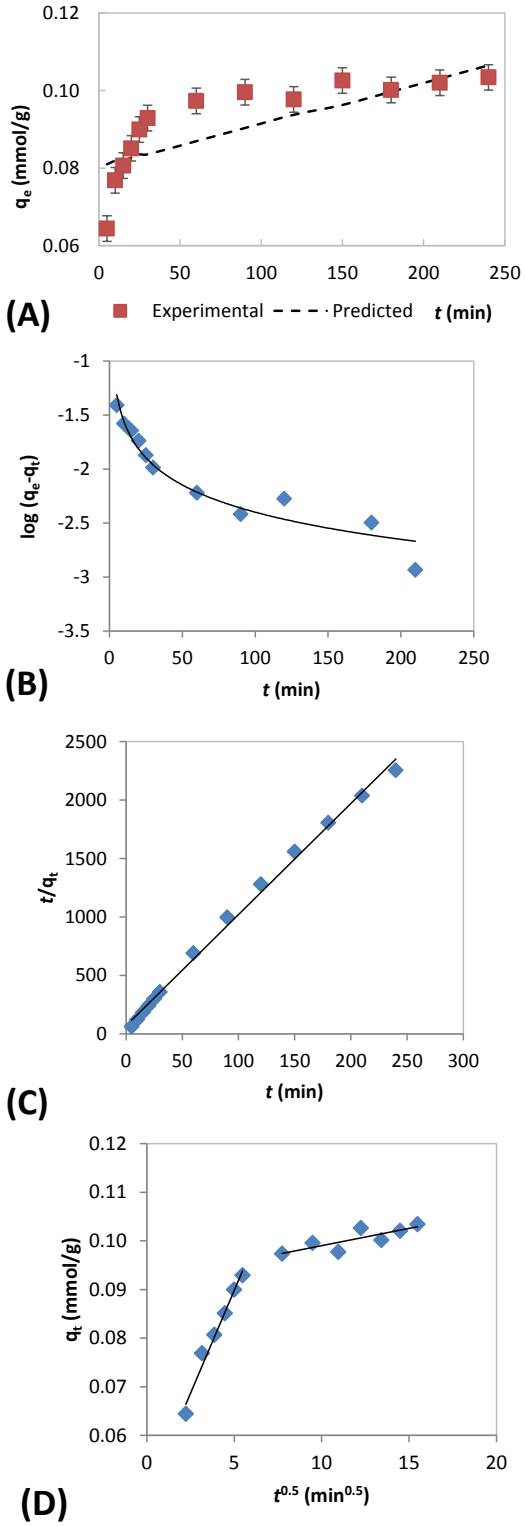

Figure 4. (A) The effect of contact time for the removal of MV using PP, and the kinetic plots of (B) Lagergren first order, (C) pseudo second order, and (D) Weber-Morris intraparticle diffusion models.

3.5 Effect of temperature and thermodynamics study

The effect of temperature ranging from 25 – 70 °C on the adsorption of MV onto PP was investigated and the adsorption capacities at different temperatures are shown in Table 2. It shows that the q_e value decreased as the temperature increased suggesting the higher temperature is less favourable for the adsorption process to occur. The thermodynamics aspect of the study was calculated using the Van't Hoff equation shown below (equation 13) in order to obtain the values of the Gibbs free energy (ΔG^o), enthalpy (ΔH^o) and entropy (ΔS^o).

$$\Delta G^O = -RTlnK \quad (13)$$

$$K = \frac{C_S}{C_e} \quad (14)$$

$$\Delta G^O = \Delta H^O - T\Delta S^O \quad (15)$$

Inserting equation 13 into equation 15

$$\ln K = \frac{\Delta S^O}{R} - \frac{\Delta H^O}{RT} \quad (16)$$

where K is the distribution coefficient for adsorption, C_S is the MV concentration adsorbed on PP (mg/L), R is the gas constant (J/mol K) and T is the absolute temperature (K).

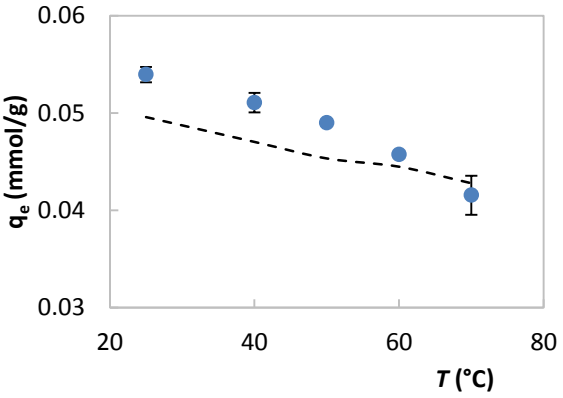

Figure 5. The effect of temperature on the adsorption of MV onto PP.

As shown in Table 2, the ΔG^o value becomes more positive as the temperature increases indicating adsorption being less spontaneous at higher temperature. Negative ΔH^o value indicates that the adsorption is exothermic in nature and negative ΔS^o

Table 2. Thermodynamics parameters for the adsorption of MV onto PP

T (°C)	T (K)	ΔG° (kJ/mol)	ΔH° (kJ/mol)	ΔS° (J/mol K)	q_e (mmol/g)
25	298	-3.15	-16.43	-44.31	0.054
40	313	-2.59			0.051
50	323	-2.20			0.049
60	333	-1.79			0.046
70	343	-1.07			0.042

value showed that the molecules' movements have less freedom. The ANN model is also in good agreement with the experimental data, predicting the same behaviour as seen in Figure 5.

3.6. Effect of dye concentration and isotherm study

Figure 6 shows the effect of increasing MV concentration on the adsorption process. It can be seen that the q_e increases as the dye concentration increased with no apparent indication of the dye uptake slowing down. ANN predicted data was in good agreement with the experimental data.

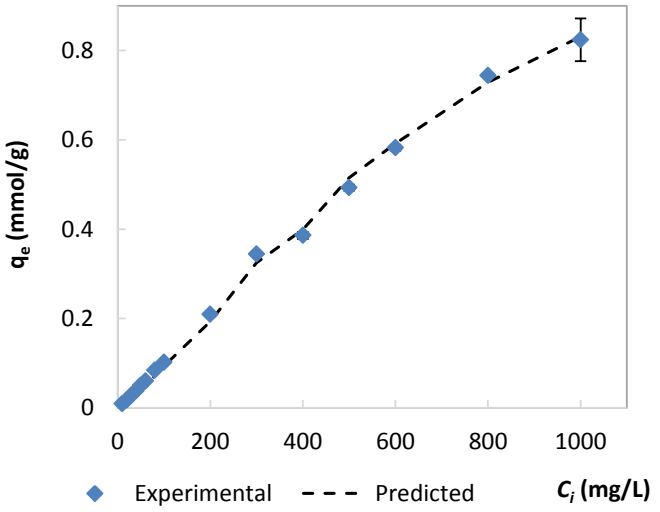

Figure 6. The effect of initial concentration on the removal of MV using PP

The experimental data was fitted into the Langmuir, Freundlich and Sips models in order to investigate the interaction between adsorbate and adsorbent during the adsorption process. The applications of the isotherm models were discussed in the literature (Foo and Hameed, 2010). From Table 3, Freundlich has the highest R^2 value (0.982) followed by Langmuir (0.968) and Sips (0.804) models while the Langmuir model has the lowest values for both EABS and χ^2 followed by Freundlich and Sips model. Through these comparisons, Sips can be considered to be the least suitable model to describe the interaction while both the Langmuir and Freundlich are both considered as better fit to the experimental data. Both the R_L and n_F values suggest that the adsorption of MV onto PP is favourable with the Langmuir q_{max} value of 1.2 mmol/g (468.3 mg/g).

Table 3. Calculated parameters of the Langmuir, Freundlich and Sips isotherm models

Models	Parameters	Values
Langmuir	q_{max} (mmol/g)	1.189
	b (L/mmol)	0.004
	R_L	0.190
	R^2	0.968
	EABS	0.229
	χ^2	0.020
Freundlich	K_F (mmol/g)	0.007
	n_F	1.235
	1/ n_F	0.810
	R^2	0.982
	EABS	0.702
	χ^2	0.235
Sips	q_{max} (mmol/g)	0.825
	K_{LF}	1.557
	K_S (L/g)	0.002
	R^2	0.804
	EABS	0.777
	χ^2	0.268

The q_{max} value is comparable to the adsorption of MV by activated carbon based on *Phragmites australis* (476.2 mg/g) (Chen et al., 2010) and superior to that of *Casuarina equisetifolia* cone (63 mg/g) (Dahri et al., 2017a), peanut straw char (101.0 mg/g)

(Xu et al., 2011), halloysite nanotube (113.6 mg/g) (Liu et al., 2011), *Azolla pinnata* (119.4 mg/g) (Kooh et al., 2015), Jackfruit seed (126.7 mg/g) (Kooh et al., 2016b), *Casuarina equisetifolia* needle (165 mg/g) (Dahri et al., 2013), soya bean waste (180.7 mg/g) (Kooh et al., 2016d), water lettuce (268.8 mg/g) (Kooh et al., 2016a), Pu-erh tea (285.7 mg/g) (Li et al., 2010), *Nepenthes rafflesiana* pitcher (288.7 mg/g) (Kooh et al. 2017a) and duckweed (332.5 mg/g) (Lim et al., 2014).

4. CONCLUSIONS

This research investigated PP as a low-cost adsorbent for the removal of MV dye. ANN model was found to be in good concurrence with the experimental data and was able to predict reasonably well. The optimum pH for MV removal using PP is at 6 which is in agreement with the concept of pH_{pzc}. The effect of ionic strength showed that dominant force of dye adsorption may be due to hydrophobic-hydrophobic interaction, instead of electrostatic interaction. The pseudo second model best described the adsorption kinetics, and indicated that the adsorption followed a second order rate law with respect to availability of adsorption sites. The Weber-Morris intraparticle diffusion model indicated that the intraparticle phase is not rate-limiting. The effect of temperature provided insights that the adsorption process of PP-MV system was both spontaneous and exothermic. Lastly, the Langmuir isotherm model best represented the adsorption process and predicted a high q_{max} value of 1.2 mmol/g (468.3 mg/g)..

REFERENCES

Argun, M.E., Güclü, D. and Karatas, M. (2014) Adsorption of Reactive Blue 114 dye by using a new adsorbent: Pomelo peel. Journal of Industrial and Engineering Chemistry, 20, 1079-1084.

Bansal, R.C. and Goyal, M. (2005) Activated carbon adsorption. CRC press.

Bhattacharyya, K.G. and Gupta, S.S. (2008) Adsorption of a few heavy metals on natural and modified kaolinite and montmorillonite: a review. Advances in colloid and interface science, 140, 114-131.

Chen, S., Zhang, J., Zhang, C., Yue, Q., Li, Y. and Li, C. (2010) Equilibrium and kinetic studies of methyl orange and methyl violet adsorption on activated carbon derived from *Phragmites australis*. Desalination, 252, 149-156.

Chong, M.N., Jin, B., Chow, C.W. and Saint, C. (2010) Recent developments in photocatalytic water treatment technology: a review. Water research, 44, 2997-3027.

Crini, G. (2006) Non-conventional low-cost adsorbents for dye removal: A review. Bioresource Technology, 97, 1061-1085.

Dahri, M.K., Kooh, M.R.R. and Lim, L.B. (2017a) Water remediation using *Casuarina equisetifolia* cone as adsorbent for the removal of methyl violet 2B dye using batch experiment method. Journal of Environment & Biotechnology Research, 6, 34-42.

Dahri, M.K., Kooh, M.R.R. and Lim, L.B.L. (2013) Removal of methyl violet 2B from aqueous solution using *Casuarina equisetifolia* needle. ISRN Environmental Chemistry, 2013, 1-8.

Dahri, M.K., Kooh, M.R.R. and Lim, L.B.L. (2014) Water remediation using low cost adsorbent walnut shell for removal of malachite green: Equilibrium, kinetics, thermodynamic and regeneration studies. Journal of Environmental Chemical Engineering, 2, 1434-1444.

Dahri, M.K., Kooh, M.R.R. and Lim, L.B.L. (2017b) Adsorption characteristics of pomelo skin toward toxic Brilliant Green dye. Scientia Bruneiana, 16, 49-56.

Demirbas, A. (2008) Heavy metal adsorption onto agro-based waste materials: a review. Journal of hazardous materials, 157, 220-229.

Fernandes, A.N., Almeida, C.A.P., Menezes, C.T.B., Debacher, N.A. and Sierra, M.M.D. (2007) Removal of methylene blue from aqueous solution by peat. Journal of Hazardous Materials, 144, 412-419.

Foo, K. and Hameed, B. (2011) Microwave assisted preparation of activated carbon from pomelo skin for the removal of anionic and cationic dyes. Chemical Engineering Journal, 173, 385-390.

Foo, K.Y. and Hameed, B.H. (2010) Insights into the modeling of adsorption isotherm systems. Chemical Engineering Journal, 156, 2-10.

Freundlich, H.M.F. (1906) Over the adsorption in solution. Journal of Physical Chemistry, 57, 385-470.

Hall, M., Frank, E., Holmes, G., Pfahringer, B., Reutemann, P. and Witten, I.H. (2009) The WEKA data mining software: an update. ACM SIGKDD Exploration Newsletter, 11, 10-18.

Hameed, B.H., Mahmoud, D.K. and Ahmad, A.L. (2008) Sorption of basic dye from aqueous solution by pomelo (*Citrus grandis*) peel in a batch system. Colloids and Surfaces A: Physicochemical and Engineering Aspects, 316, 78-84.

Hanafiah, M.A.K.M., Ngah, W.S.W., Zolkafly, S.H., Teong, L.C. and Majid, Z.A.A. (2012) Acid Blue 25 adsorption on base treated *Shorea dasyphylla* sawdust: Kinetic, isotherm, thermodynamic and spectroscopic analysis. Journal of Environmental Sciences, 24, 261-268.

Ho, Y.S. and McKay, G. (1998) Sorption of dye from aqueous solution by peat. Chemical Engineering Journal, 70, 115-124.

Hu, Y., Guo, T., Ye, X., Li, Q., Guo, M., Liu, H. and Wu, Z. (2013) Dye adsorption by resins: Effect of ionic strength on hydrophobic and electrostatic interactions. Chemical Engineering Journal, 228, 392-397.

Kooh, M.R.R., Dahri, M.K. and Lim, L.B.L. (2016a) Jackfruit seed as a sustainable adsorbent for the removal of Rhodamine B dye. Journal of Environment & Biotechnology Research, 4, 7-16.

Kooh, M.R.R., Dahri, M.K. and Lim, L.B.L. (2016b) The removal of rhodamine B dye from aqueous solution using *Casuarina equisetifolia* needles as adsorbent. Cogent environmental science, 2, 1140553.

Kooh, M.R.R., Dahri, M.K. and Lim, L.B.L. (2017a) Removal of methyl violet 2B dye from aqueous solution using *Nepenthes rafflesiana* pitcher and leaves. Applied Water Science, DOI: 10.1007/s13201-017-0537-1.

Kooh, M.R.R., Dahri, M.K., Lim, L.B.L. and Lim, L.H. (2016c) Batch adsorption studies on the removal of Acid Blue 25 from aqueous solution using *Azolla pinnata* and soya bean waste. Arabian Journal for Science and Engineering, 41, 2453-2464.

Kooh, M.R.R., Dahri, M.K., Lim, L.B.L., Lim, L.H. and Malik, O.A. (2016d) Batch adsorption studies of the removal of methyl violet 2B by soya bean waste: isotherm, kinetics and artificial neural network modelling. Environmental Earth Sciences, 75, 1-14.

Kooh, M.R.R., Lim, L.B.L., Dahri, M.K., Lim, L.H. and Sarath Bandara, J.M.R. (2015) *Azolla pinnata*: An efficient low cost material for removal of Methyl Violet 2B by using adsorption method. Waste and Biomass Valorization, 6, 547-559.

Kooh, M.R.R., Lim, L.B.L., Lim, L.H. and Bandara, J.M.R.S. (2016e) Batch adsorption studies on the removal of malachite green from water by chemically modified *Azolla pinnata*. Desalination and Water Treatment, 57, 14632-14646.

Kooh, M.R.R., Lim, L.B.L., Lim, L.H. and Dahri, M.K. (2016f) Phytoremediation capability of *Azolla pinnata* for the removal of malachite green from aqueous solution. Journal of Environment and Biotechnology Research, 5, 10-17.

Kooh, M.R.R., Lim, L.B.L., Lim, L.H. and Dahri, M.K. (2016g) Separation of toxic rhodamine B from aqueous solution using an efficient low-cost material, *Azolla pinnata*, by adsorption method. Environmental Monitoring and Assessment, 188, 1-15.

Kooh, M.R.R., Muhammad Khairud, D., Lim, L.B.L. and Lim, L.H. (2017b) Remediation of direct blue 71 wastewater by salting out processes using inorganic salt solutions and seawater. Journal of Environment & Biotechnology Research, 6, 53-57.

Lagergren, S. (1898) About the theory of so called adsorption of soluble substances. Kungliga Svenska vetenskapsakademiens handlingar, 24, 1-39.

Langlais, B., Reckhow, D.A. and Brink, D.R. (1991) Ozone in water treatment: application and engineering. Paris, France: CRC press.

Langmuir, I. (1918) The adsorption of gases on plane surfaces of glass, mica and platinum. Journal of the American Chemical Society, 40, 1361-1403.

Li, P., Su, Y.J., Wang, Y., Liu, B. and Sun, L.M. (2010) Bioadsorption of methyl violet from aqueous solution onto Pu-erh tea powder. Journal of hazardous materials, 179, 43-48.

Liang, J., Wu, J., Li, P., Wang, X. and Yang, B. (2012) Shaddock peel as a novel low-cost adsorbent for removal of methylene blue from dye wastewater. Desalination and Water Treatment, 39, 70-75.

Lim, L.B.L., Priyantha, N., Chan, C.M., Matassan, D., Chieng, H.I. and Kooh, M.R.R. (2014) Adsorption behavior of Methyl Violet 2B using duckweed: Equilibrium and kinetics studies. Arabian Journal for Science and Engineering, 39, 6757-6765.

Lim, L.B.L., Priyantha, N., Chan, C.M., Matassan, D., Chieng, H.I. and Kooh, M.R.R. (2016) Investigation of the sorption characteristics of water lettuce (WL) as a potential low-cost biosorbent for the removal of methyl violet 2B. Desalination and Water Treatment, 57, 8319-8329.

Liu, R., Zhang, B., Mei, D., Zhang, H. and Liu, J. (2011) Adsorption of methyl violet from aqueous solution by halloysite nanotubes. Desalination, 268, 111-116.

Luo, J., Ge, J.-w., Yang, X.-b. and Li, X.-d. (2010) Adsorption Kinetics of modified pomelo peel cellulose towards lead ions. Journal of Food Science, 3, 18.

Özacar, M. and Şengil, İ.A. (2004) Application of kinetic models to the sorption of disperse dyes onto alunite. Colloids and Surfaces A: Physicochemical and Engineering Aspects, 242, 105-113.

Peralta-Hernández, J., Meas-Vong, Y., Rodríguez, F.J., Chapman, T.W., Maldonado, M.I. and Godínez, L.A. (2006) In situ electrochemical and photo-electrochemical generation of the fenton reagent: A potentially important new water treatment technology. Water research, 40, 1754-1762.

Renault, F., Morin Crini, N., Gimbert, F., Badot, P.-M. and Crini, G. (2008) Cationized starch-based material as a new ion-exchanger adsorbent for the removal of C.I. Acid Blue 25 from aqueous solutions. Bioresource Technology, 99, 7573-7586.

Saikaew, W., Kaewsarn, P. and Saikaew, W. (2009) Pomelo peel: agricultural waste for biosorption of cadmium ions from aqueous solutions. World academy of science, engineering and technology, 56, 287-291.

Samiey, B. and Toosi, A.R. (2010) Adsorption of malachite green on silica gel: Effects of NaCl, pH and 2-propanol. Journal of Hazardous Materials, 184, 739-745.

Sips, R. (1948) Combined form of Langmuir and Freundlich equations. Journal of Chemical Physics, 16, 490-495.

Tasaso, P. (2014) Adsorption of copper using pomelo peel and depectinated pomelo peel. Journal of Clean Energy Technologies, 2, 154-157.

Taty-Costodes, V.C., Fauduet, H., Porte, C. and Delacroix, A. (2003) Removal of Cd(II) and Pb(II) ions, from aqueous solutions, by adsorption onto sawdust of *Pinus sylvestris*. Journal of hazardous materials, 105, 121-142.

Vijayaraghavan, K. (2016) Biosorption of metals: a complete handbook. Chennai, India: Vinanie Publishers.

Wang, L.K., Shammas, N.K. and Hung, Y.-T. (2010) Advanced biological treatment processes. Springer Science & Business Media.

Weber, W. and Morris, J. (1963) Kinetics of adsorption on carbon from solution. Journal of the Sanitary Engineering Division, 89, 31-60.

Xu, R.k., Xiao, S.c., Yuan, J.h. and Zhao, A.z. (2011) Adsorption of methyl violet from aqueous solutions by the biochars derived from crop residues. Bioresource Technology, 102, 10293-10298.